

Effect of Various Supports on the Physico-chemical Properties of V-Sb Oxides in the Oxidative Dehydrogenation of Isobutane

N. T. Shamilov* and V. P. Vislovskiy†

Department of Chemistry of Baku State University, Baku, 1148 Azerbaijan. *E-mail: kimya@mail.ru

†Institute of Chemical Problems, Azerbaijan National Academy of Sciences, 29 H. Javid ave.,
370143 Baku, Azerbaijan

(Received May 30, 2011; Accepted July 7, 2011)

ABSTRACT: $V_{0.9}Sb_{0.1}O_x$ systems, bulk and deposited on different supports (five types of γ -aluminas, α -alumina, silica-alumina, silica gel, magnesium oxide), have been tested in the oxidative dehydrogenation (ODH) of iso-butane. This statement is derived from the data obtained by a set of characterisation techniques (specific surface area measurements, X-ray diffraction, X-ray photoelectron spectroscopy, laser Raman spectroscopy, *in situ* differential scanning calorimetry and *in situ* diffuse reflectance-absorption infrared Fourier transform spectroscopy).

Key words: Vanadium-antimony oxide catalysts, Supports, Oxidative dehydrogenation, Isobutane, Isobutene

INTRODUCTION

Vanadium oxide-based systems are well-established catalysts for the partial oxidation, ammoxidation and oxidative dehydrogenation (ODH) of hydrocarbons into valuable oxygenates, nitriles and olefins.¹⁻¹⁵ Most of these catalysts are deposited on the surface of an oxide support, such as SiO_2 , Al_2O_3 , TiO_2 , and ZrO_2 .^{9,16} Catalytic performance of vanadium oxide-based catalysts in the above reactions is known to be highly dependent on the nature of the support and its interaction with active phases, as well as on the loading of an active component. Depending mainly on these factors, deposition of vanadia onto oxide supports can result in isolated vanadium ions, small clusters, or polymeric species, two-dimensional vanadium oxide chain, crystalline or amorphous three-dimensional vanadium oxide or mixed oxide phases with a material of support, or any combination of these structures.^{9,16} The method of preparation does not significantly affect the structure of supported vanadia species; however, it affects the vanadium oxide dispersion.^{9,16,17} Up until now, no consistent model can describe the role of the structure/composition of supported oxides, especially in the presence of certain dopants.¹⁶ Estimation of the relative reactivities of different supported vanadium oxide species is still a more complex problem and is the subject of broad debate.

In this paper, we compare the physico-chemical properties of bulk and supported V-Sb oxides for the isobutane ODH. A set of characterisation techniques has been uti-

lised to elucidate how the nature of a support and the loading of V-Sb oxide affect the state of active component. X-ray diffraction (XRD) and X-ray photoelectron spectroscopy (XPS) were used to characterise phase and surface compositions, respectively. *In situ* differential scanning calorimetry (DSC) was applied to study the intensity of interactions between V-Sb oxide and support materials. *In situ* diffuse reflectance-absorption infrared Fourier transform spectroscopy (DRIFTS) and laser Raman spectroscopy (LRS) were employed to reveal further details on this interaction and on the nature of active VO_x -component.

EXPERIMENTAL

Catalyst Characterisation

BET specific surface area (SSA) measurements were performed with a Micrometrics Flow Sorb II 2300 instrument by adsorption of N_2 at liquid nitrogen temperature on samples previously outgassed at 150 °C for 1 h.

XRD patterns were obtained with a high resolution X-ray Kristalloflex 805 (Siemens) diffractometer equipped with a Siemens D-5000 detector using Ni-filtered $CuK\alpha$ -radiation. Powdered samples were analyzed without any pre-treatment after deposition on a quartz single crystal sample holder.

Laser Raman spectra were recorded using Labram integrated Raman system (Dilor). The system consists of a microscope coupled confocally to a 300 mm focal length spectrograph. The excitation wave is supplied by an inter-

nal 20 mW HeNe laser. The sample was placed on a glass plate in the microscope field of vision. Then the laser was focused on the sample and the spectrum was recorded with selected acquisition time and accumulation number.

XPS analysis was performed with an SSX-100 model 206 (Surface Science Instruments, SSI) X-ray photoelectron spectrometer. Monochromatic X-rays produced by an Al anode ($AlK_{\alpha}=1487.6$ eV) were focused in an area of about 1.4 mm^2 . Pressed powder samples were placed into small troughs. The binding energy (BE) values were referred to the adventitious C1s peak at 284.8 eV. The intensities were estimated by calculating the integral of each peak after subtraction of the “S-shaped” background. Atomic concentration (AC) of each element was calculated using a conventional procedure suggested by the instrument manufacturer (SSI).

In order to study the vanadium oxide spreading over the support (alumina, silica gel) the real XPS intensity ratios (I_V/I_{Al} or I_V/I_{Si}) were compared with those calculated theoretically for a monolayer formation (I_V^0/I_{Al}^0 or I_V^0/I_{Si}^0) using the following equation suggested by Kerkhof and Moulijn¹²:

$$\frac{I_V^0}{I_{Al}^0(I_{Si}^0)} = \frac{N_V D_V \sigma_V}{N_{Al(Si)} D_{Al(Si)} \sigma_{Al(Si)}} \times \frac{1}{\rho_{Al(Si)} S_{Al(Si)} \lambda_{Al(Si)}} \times \frac{(1 + \exp(-2/\rho_{Al(Si)} S_{Al(Si)} \lambda_V))}{(1 - \exp(-2/\rho_{Al(Si)} S_{Al(Si)} \lambda_V))}$$

where

$\rho_{Al}=3.5\text{ g/cm}^3$ -density of alumina, $\rho_{Si}=2.3\text{ g/cm}^3$ -density of silica gel;

S_i - specific surface area of the support; N_V/N_i -atomic ratio of the elements representative of the supported V_2O_5 and the support;

σ_i - photoelectron cross section values ($\sigma_{V\ 2p3}=6.37$, $\sigma_{Al\ 2p}=0.5371$, $\sigma_{Si\ 2p}=0.817$)¹³;

λ_i - photoelectron escape depths: $\lambda_{V\ 2p3}=15.2\text{ nm}$, $\lambda_{Al\ 2p}=20.1\text{ nm}$ (for Al_2O_3); $\lambda_{V\ 2p3}=18.8\text{ nm}$, $\lambda_{Si\ 2p}=24.5\text{ nm}$ (for SiO_2)¹⁴;

D_i - spectrometer detection efficiencies for the corresponding photoelectrons, calculated according to¹⁵:

$$D=E_a (E_d/E_k)^n,$$

where

$$n = 0.5594 + 0.6072 \log(E_d/E_k) + 0.3309 \log^2(E_d/E_k);$$

$$E_a = 150\text{ eV};$$

$$E_k = h\nu - E_b = 1486.6 - E_b;$$

$$E_b(Al\ 2p) = 74.5\text{ eV}, E_b(V\ 2p3) = 517\text{ eV}.$$

Thermal effects that accompany interactions between supported oxides and support materials were studied using a DSC-111 Differential Scanning Calorimeter (Setaram). Bulk V-Sb oxide and support material were ground separately in a mortar, mixed, pressed into pellets and placed into a flow quartz cell inside the calorimetric block. Measurements were performed at linear heating (10 K/min) after a 1 h drying of the sample in an air flow. Details of experimental setup and procedures are published elsewhere.¹⁶

Diffuse reflectance-absorption infrared Fourier transform (DRIFT) spectra were recorded by an IFS 88 Bruker FT spectrophotometer (resolution 4 cm^{-1}). The *in situ* DRIFTS cell consisted of cup-shaped ceramic oven with porous bottom and thermocouple, water-cooled shell with ZnSe glasses, gas inlet and outlet tubes. The spectra were recorded in absorbance mode. The spectrum of a gas phase recorded with an aluminum mirror placed into the sample position was used as a background while recording spectra of solid samples for subtracting the bands corresponding to gaseous water, CO_2 and hydrocarbons. Baseline corrections and other treatments of spectra were carried out using the driving OPUS software. In most cases 200 scans were accumulated. Usually, before reaction and adsorption measurements, samples were heated in a DRIFTS cell to $500\text{ }^\circ\text{C}$ in a helium flow, calcined at $500\text{ }^\circ\text{C}$ in an air flow and cooled down in a helium flow to the temperature of experiment. Spectra of wet samples were recorded without this pre-treatment. Ammonia adsorption was carried out for 30 min at $150\text{ }^\circ\text{C}$ on pre-heated samples from a $5\%NH_3$ - $95\%He$ mixture flow. Spectra were recorded after desorption of excess ammonia for 20 min at $150\text{ }^\circ\text{C}$ in a helium flow.

RESULTS AND DISCUSSION

In our recent paper,¹⁷ we reported the conversion of isobutane to iso-butene on different supports (five types of γ -aluminas, α -alumina, silica-alumina, silica gel, magnesium oxide). It has been found that specific surface areas (SSA) of the supported catalysts are lower than that of the starting supports (Tables 1 and 2).¹⁷

According to our XRD data,¹⁷ the main phase of fresh, bulk VSb oxide sample is of formal composition $V_{0.9}Sb_{0.1}O_x$ is V_2O_5 (shcherbinaite); a small amount of the $V_{1.1}Sb_{0.9}O_4$ phase is also present in this system. Well-crystallized V_2O_5 -phase is also observed over silica-containing supports (SG, SA) (see Fig. 1¹⁷). However, for all systems containing up to 1 ML of active component over γ -alu-

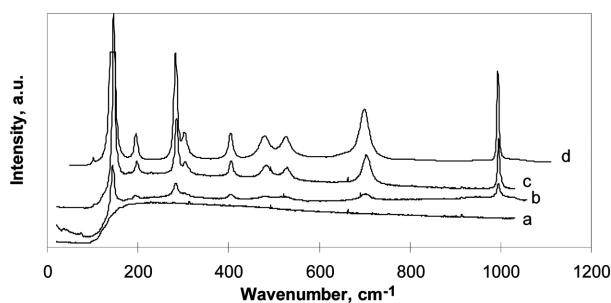


Fig. 1. Raman spectra of catalysts: (a) 0.5VSb/A(wa), (b) 1VSb/A(wa), (c) 2VSb/A(wa), and (d) reference bulk V_2O_5 .

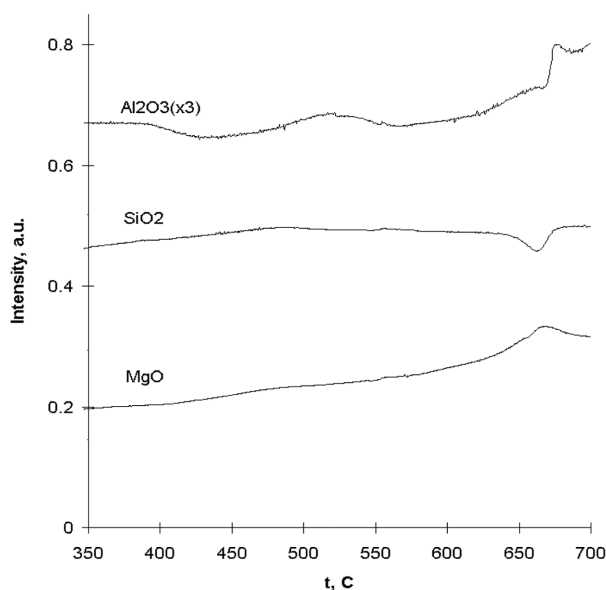


Fig. 2. The DSC recorded thermal effects upon heating of the mechanical mixtures of VSb-oxide component with supports: A(wa), SG, and M.

minas, no well-crystallized V-containing phases are observed (Fig. 2¹⁷). Noticeable amounts of V_2O_5 phase were found only when the formal coverage reaches 2 ML (Fig. 2¹⁷). No crystalline phase of mixed vanadium-antimony oxide was found in these catalysts.

Fig. 1 shows Raman spectra of nVSb/A (wa) samples along with the spectrum of reference bulk V_2O_5 . No Raman bands were observed for 0.5VSb/A(wa), while in 1VSb/A(wa) and 2VSb/A(wa) samples the bands attributed to V_2O_5 were found. No indication for the presence of any other forms of supported vanadium or antimony oxide can be found in the Raman spectra.

The results of XPS measurements are summarized in Table 1, where the values of electron binding energy (BE) for vanadium and antimony, as well as V/Sb, V/Al, (or/ and V/Si) and Sb/Al (or/and Sb/Si) atomic ratios are presented. BE values of $Sb3d_{3/2}$ in all samples are very similar. On the contrary, the BE of $V2p_{3/2}$ in the bulk system is significantly lower than in supported catalysts, indicating a lower oxidation degree of vanadium. The comparison of surface V/Sb atomic ratio evaluated from the XPS data for the unsupported sample (2.2) with its bulk composition (V/Sb=8.8) indicates that the surface is strongly enriched with antimony.

Comparison of the surface V/Al and Sb/Al ratios with nominal ones for 1VSb/aA catalyst shows that the surface is strongly enriched in both vanadium (by a factor of 5) and especially in antimony (by a factor of 9). The measured V/Sb ratio on the surface of α -alumina is lower than the nominal one. The surfaces of catalysts over silica-containing supports are impoverished in both V and Sb (compared to measured and nominal values of V/Si, Sb/Si, as well as V/Al and Sb/Al ratios for SA- and SG-supported

Table 2. Calculated and experimental values of XPS I_V/I_{Al} and I_V/I_{Si} ratios for VSb/A(wa), VSb/A(b) and VSb/SG catalysts

Support	Loading, n	I_V/I_{Al} or I_V/I_{Si}	
		Calcul.	Exper.
A(wa)	0.5	0.928	0.823
	1	1.86	1.60
A(b)	0.5	0.931	0.674
	1	1.86	1.404
SG	1	2.45	0.719

Table 1. XPS characteristics of 1VSb/support and bulk VSb oxide systems

Catalyst (VSb/support)	Binding Energy (eV)		Atomic ratio					
			V/Sb		V/Al (V/Si)		Sb/Al (Sb/Si)	
	$V2p_{3/2}$	$Sb3d_{3/2}$	measured	nominal	measured	nominal	measured	nominal
Bulk VSb	516.7	540.1	2.2	8.8	-	-	-	-
/ γ A(wa)	517.2	539.8	7.7	8.8	0.154	0.112	0.020	0.013
/ γ A(b)	517.1	539.9	7.2	8.8	0.172	0.105	0.024	0.012
/ γ A(ms)	517.3	540.1	8.9	8.8	0.088	0.068	0.010	0.008
/ α A	516.9	539.9	4.9	8.8	0.141	0.029	0.029	0.003
/SA	517.4	539.9	19.1	8.8	0.926 (0.385)	2.22 (0.476)	0.048 (0.020)	0.256 (0.054)
/SG	517.2	540.2	15.4	8.8	(0.118)	(0.250)	(0.008)	(0.029)

samples), but the surface V/Sb ratio values are higher than nominal.

All γ -alumina-supported samples display surface V/Sb ratios much closer to the nominal value; in the case of 1VSb/Al(ms), the measured and nominal values are practically equal.

Table 2 shows the I_V/I_{Al} ratios measured for the samples on A(wa), A(b) and SG in comparison with the theoretically estimated values (see section 2.3) for monolayer coverage of the support.

One can see that although I_V/I_{Al} ratio does not reach the theoretical value, real vanadium oxide distribution on γ -aluminas is close to monolayer spreading. For 1VSb/SG catalyst this distribution is much worse: the experimental value is much lower than the theoretical one.

Thermal effects recorded at heating of mechanical mixtures of bulk VSb oxide and support materials measured by DSC (Fig. 2) reflect types of interactions that take place in supported systems.

Bulk V_2O_5 -like VSb oxide melts at $\sim 670^\circ\text{C}$; if a corresponding endothermic effect is observed, this is an indication of the absence of any significant interaction between two components. This is what is found in the case of the $VSbO_x$ -SG mechanical mixture. By contrast, in the case of the $VSbO_x$ -A(ms) mixture, two exothermal effects are observed - a broad one in the range of 510 – 550°C and a sharp one at $\sim 700^\circ\text{C}$. Upon heating the $VSbO_x$ -MgO mixture, a broad exothermal effect appears above 400°C and reaches the maximum at about 670°C . These exotherms suggest the high affinity between components in both systems.

In situ DRIFT spectra of A(wa), bulk V_2O_5 and Sb_2O_4 , as well as bulk V-Sb oxide (not presented here) were recorded preliminarily to obtain the reference bands for characterisation of VSb/A(wa) systems. In the spectrum of A(wa) at room temperature, broad bands assigned to $\nu(\text{OH})$ at 2800 – 3700 cm^{-1} , $\delta(\text{OH})$ from adsorbed water at 1638 cm^{-1} and $\delta(\text{O-H})$ in the bulk at 1000 – 1100 cm^{-1} .¹⁸ were observed. In the spectrum of V_2O_5 , bands at 1040 , 1000 , 940 cm^{-1} assigned to $\nu(\text{V=O})$ vibrations¹⁹ were detected as well as two bands at 2020 and 1970 cm^{-1} which correspond to overtones of $\nu(\text{V=O})$ vibrations.^{20,21} In the spectrum of Sb_2O_4 the bands are present at 820 and 680 cm^{-1} . The spectrum of bulk VSb oxide contains bands at 2020 , 1970 , 1040 and 940 cm^{-1} assigned to $\nu(\text{V=O})$ vibrations. This spectrum is similar to that of V_2O_5 ; the addition of antimony affects only the band near 1000 cm^{-1} .

In the spectrum of 1VSb/A(wa) (not shown), the $\nu(\text{O-H})$ bands at 2800 – 3700 cm^{-1} , and $\delta(\text{O-H})$ at 1640 cm^{-1} ,

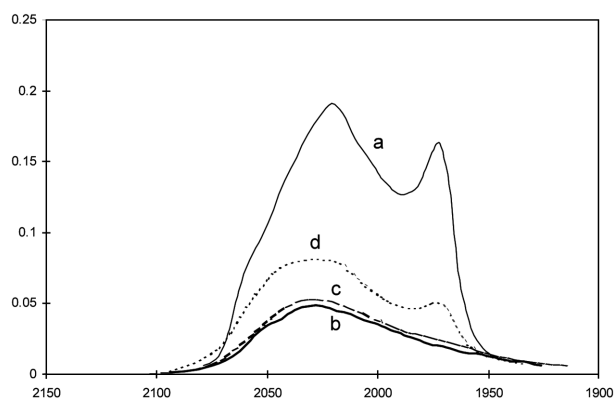


Fig. 3. DRIFT spectra ($\nu(\text{V=O})$ overtone region) of (a) reference bulk V_2O_5 , (b) 0.5VSb/A(wa), (c) 1VSb/A(wa), and (d) 2VSb/A(wa).

1000 – 1100 cm^{-1} and 2020 – 1970 cm^{-1} are observed. The band at 1000 – 1100 cm^{-1} originates from a superimposition of bands $\nu(\text{V=O})$ ¹⁹ and $\delta(\text{O-H})$ in bulk Al_2O_3 . As the main band of $\nu(\text{V=O})$ vibrations at 1000 cm^{-1} overlaps with that of the alumina support, weak bands at 2020 – 1970 cm^{-1} , the overtones of $\nu(\text{V=O})$ vibrations,^{20,21} were used to identify the presence of vanadium oxide on alumina.

The spectra of supported samples and pure bulk V_2O_5 (used as a reference) in the region of $\nu(\text{V=O})$ overtones are presented in Fig. 3. For the bulk sample, two bands at 2020 and 1970 cm^{-1} are detected whereas for 0.5VSb/A(wa) sample only one band around 2030 cm^{-1} is observed. A band at 1975 cm^{-1} appears in the spectrum of 1VSb/A(wa) and becomes more intense in the case of 2VSb/A(wa). It was suggested that band at 2020 – 2030 cm^{-1} can be attributed to a monolayer form of vanadium oxide whereas the band at 1975 cm^{-1} corresponds to larger three-dimensional clusters of vanadium oxide.

Adsorbed water was present on fresh samples and decreased the intensities of $\nu(\text{V=O})$ overtone. Intensities of the band at 2020 cm^{-1} in the spectra recorded in “wet” conditions (ambient atmosphere), I_w , were compared to those recorded after dehydroxylation in the DRIFTS cell in a dry air flow at 500°C for 0.5 h and cooling to 20°C (“dry” conditions, I_d). Adsorbed water decreases the intensities of the band corresponding to an $\nu(\text{V=O})$ overtone due to an interaction with a surface vanadyl groups. This is the reason why the I_w/I_d ratio reflects the fraction of bulk V=O groups in a total number of such species in a “dry” sample. The relative amount of V=O species at the surface of VSb/A(wa) catalysts (estimated by I_w/I_d ratios) decreases with increasing of V-Sb-O loading: almost all

V=O bonds of 0.5VSb/A(wa) catalyst with low loading of supported V-Sb-O component were accessible for adsorbed water ($I_w=0$). This is indicative for the formation of a monolayer of the VSb oxide on the support surface. At increasing VSb oxide loading, the fraction of V=O groups accessible for adsorbate decreases: 79% of V-atoms in 1VSb/A(wa) and ca. 56% of those in 2VSb/A(wa) catalysts are exposed at the surface. This could be due to the formation of three-dimensional VSb oxide structures (polylayers, bulky clusters).

Adsorption of ammonia was studied to reveal possible differences in the nature of the surface of the catalysts. The spectrum of ammonia adsorbed on the bare A(wa) support (Fig. 4) shows bands at 1685, 1622, 1481, 1263 cm^{-1} . Those at 1685, 1481 cm^{-1} are attributed to the vibrations of ammonium ion formed as a result of adsorption of ammonia on Brönsted acid sites. Bands at 1622 and 1263 cm^{-1} are assigned to the coordinated ammonia adsorbed on Lewis acid sites.¹⁸ The band at 1400 cm^{-1} corresponds to ammonium ions formed on glass walls of the DRIFTS cell.

In the spectrum of ammonia adsorbed on bulk V-Sb-O sample (see Fig. 4), an intense band at 1420 cm^{-1} corresponds to ammonium ions. The band of coordinated ammonia at 1250 cm^{-1} is very weak. Similar results were reported for the ammonia adsorption on bulk V_2O_5 .^{22,23}

The increase of VSb-loading in VSb/A(wa) samples results in the progressive shift of the ammonium ion band frequency from 1440 to 1427–1423 cm^{-1} and in the increase of its intensity. At the same time, the coordinated ammonia band becomes slightly displaced from 1257 to

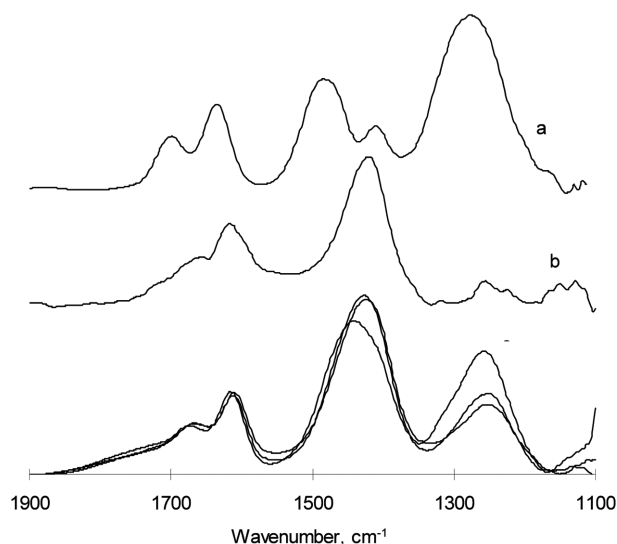


Fig. 4. DRIFT spectra of ammonia adsorbed on (a) A(wa), (b) bulk VSb oxide, (c) 0.5VSb/A(wa), (d) 1VSb/A(wa), and (e) 2VSb/A(wa).

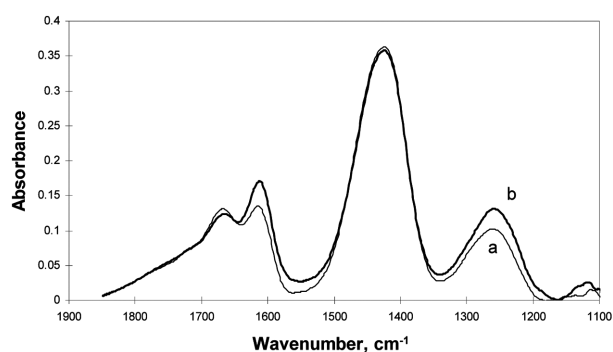


Fig. 5. DRIFT spectra of ammonia adsorbed on 1VSb/A(wa) sample after treatment at 550 °C in flow of (a) air and (b) nitrogen.

1251 cm^{-1} . The ratio of the intensities of the bands corresponding to Lewis acid sites in the catalyst and in the support spectra, $I_{L(cat)}/I_{L(A(wa))}$ decreases from 0.7 for 0.5 VSb/Al (wa) to 0.45 for 1VSb/A (wa) and to 0.4 for 2VSb/A (wa). These changes are likely due to the increasing coverage of pure alumina Lewis acid centers with V-Sb oxide, which shows mainly Brönsted acidity. Bands of coordinated ammonia adsorbed on Lewis acid sites were, however, rather intense even at high V-Sb-O loading indicating that patches of the support surface remained uncovered by a supported component.

Fig. 5 presents the spectra of ammonia adsorbed at 150 °C on 1VSb/A(wa) samples pre-treated in a DRIFTS cell at 550 °C for 0.5 h in dry air (curve a) and nitrogen (curve b) flows. One can see that treatment with an inert gas does not affect bands assigned to ammonium ions but slightly alters the intensity of the bands associated with coordinated ammonia. Apparently, a certain number of Lewis acid sites can form due to a partial loss of oxygen during such treatment. Intensity of the band at 1260 cm^{-1} assigned to this form, however, is lower than the one associated with Lewis sites on uncovered Al_2O_3 surface (Fig. 4).

DISCUSSION

DRIFTS and Raman spectroscopic data provide us further details on the interaction between VSb-oxide and γ - Al_2O_3 supports. They indicate that only a monolayer form of vanadium oxide exists in the 0.5VSb/gA sample. According to the behavior of the DRIFTS band at 1975 cm^{-1} and Raman spectra, larger clusters of VSb oxide begin to form in the catalysts with formal coverages of 1 and 2 monolayers. Almost all V=O bonds of monolayer vanadium oxide are able to interact with ambient water, whereas only part of V=O bonds of the larger clusters of

V-Sb-O component are accessible for water. The fraction of these active bonds is gradually decreased with increased V-loading. A similar effect was observed in.^{24,25} It is more difficult to come to unambiguous conclusions from the ammonia adsorption data, despite this question being extensively studied by IR spectroscopy on bulk and supported vanadium oxides (see, for instance,^{22,23,26-28}). Here, some authors state that ammonia is mainly adsorbed on the surface of bulk vanadium oxide as ammonium ions on Brönsted centers.^{22,23} When ammonia was adsorbed on V_2O_5/Al_2O_3 , the band of coordinated ammonia disappeared when the V_2O_5 content was increased up to 25 mol% (2-4 ML).²⁶ That is why authors concluded that coordinated ammonia is observed only on uncovered Al_2O_3 surfaces and that the presence of this band testifies the incomplete covering of alumina due to agglomeration of vanadium oxide on the support surface. However, based on similar observations, Khader²⁷ concluded that some part of coordinated ammonia was chemisorbed on supported vanadium oxide.

Our experiments showed the presence of both Lewis and Brönsted acid sites on the alumina support surface, and only Brönsted sites on unsupported V-Sb-O sample. Consequently, the impregnation of alumina with the active component decreases the number of Lewis sites and brings new Brönsted centers. We observed here that the increase of V-Sb-O-loadings on γ -alumina weakens the spectral features which are characteristic for coordinated form of ammonia on the Lewis acid sites and strengthens the features inherent to the adsorption of ammonia on Brönsted acid sites, which must correspond to the V-Sb-O supported component. However, the disappearance of Lewis sites is not complete even for the sample with 2 ML formal coverage. This could be due to two reasons: i) while increasing the loading, a partial agglomeration of supported phase takes place and some part of alumina surface remains uncovered; ii) at a variance of the surface of bulk V-Sb oxide, which has practically only Brönsted acidity, the surface of VSb oxide supported on γ -alumina might contain a substantial amount of Lewis acid sites.

Under an inert gas flow, vanadium oxide evolves a significant part of surface oxygen²⁹ thus creating the centers of Lewis acidity (V-ions of low coordination). This treatment of our alumina-supported VSb oxide catalysts increases only slightly the intensity of the bands of coordinated ammonia (Fig. 5). Apparently, only a limited number of Lewis acid sites might be present on a partially reduced surface of supported V-Sb-O phase. Thus, a part of γ - Al_2O_3

support surface does remain uncovered. This is consistent with other results (DSC, DRIFTS) discussed above.

CONCLUSION

$V_{0.9}Sb_{0.1}O_x$ systems, bulk and deposited on different supports (five types of γ -alumina, α -alumina, silica-alumina, silica gel, magnesium oxide), have been tested in the oxidative dehydrogenation (ODH) of iso-butane. Catalytic performance of V-Sb oxides is shown to be dependent on the supporting and the nature of the support decreasing in a series: γ - $Al_2O_3 > \alpha$ - $Al_2O_3 > Si$ - Al - $O > SiO_2$ $MgO \gg$ unsupported. It was determined that the best catalytic effect of $V_{0.9}Sb_{0.1}O_x/\gamma$ - Al_2O_3 compared with other systems associated with the optimal interaction between the surfaces of components and surface of the carrier. Because of this, it should be noted that at this time formed amorphous active VO_x components with a high degree of oxidation of vanadium. This statement is derived from the data obtained by a set of characterisation techniques (specific surface area measurements, X-ray diffraction, X-ray photoelectron spectroscopy, laser Raman spectroscopy, *in situ* differential scanning calorimetry and *in situ* diffuse reflectance-absorption infrared Fourier transform spectroscopy).

REFERENCES

1. Kung, H. J. *Adv. Catal.* **1994**, 40, 1.
2. Mamedov, E. A.; Cortes Corberan, V. J. *Appl. Catal. A.* **1995**, 127, 1.
3. Rizayev, R. G.; Mamedov, E. A.; Vislovskii, V. P.; Sheinin, V. E. *J. Appl. Catal. A.* **1992**, 83, 103.
4. Albonetti, S.; Cavani, F.; Trifirò, F., *Catal. Rev. -Sci. Eng.* **1996**, 38, 413.
5. Delmon, B.; Ruiz, P.; Carrazan, S. R. G.; Korili, S.; Vicente Rodriguez, M. A.; Sobalik, Z. *Stud. Surf. Sci. Catal.* **1996**, 100, 1.
6. Haber, J.; in: Ertl, G.; Knözinger, H.; Weitkamp, J., *Handbook of Heterogeneous Catalysis*: VCH Weinheim. 1997; Vol. 5, p 2253.
7. Blasco, T. M.; López Nieto, J. M. *J. Appl. Catal. A.* **1997**, 157, 117.
8. Grzybowska-Swierkosz, B. *J. Appl. Catal. A.* **1997**, 157, 409.
9. Kung, H. H.; Kung, M. C. *J. Appl. Catal. A.* **1997**, 157, 105.
10. Weckhuysen, B. M.; Keller, D. E. *Catal. Today.* **2003**, 78, 25.
11. Murakami, T.; Inomata, M.; Mori, K.; K. Suzuki, T. Ui; Miyamoto, A.; Hattori, T.; *Stud. Surf. Sci. Catal.* **1983**, 16, 531.

12. Kerkhof, F. P. J.; Moulijn, J. A.; *J. Phys. Chem.* **1979**, *83*, 1612.
 13. Scofield, J. H. *J. Electron Spectrosc. Relat. Phenom.* **1976**, *8*, 129.
 14. Szajman, J.; Liesegang, J.; Jenkin, J. G.; Leckey, R. C. G.; *J. Electron Spectrosc. Relat. Phenom.* **1983**, *23*, 97.
 15. Weng, L. T.; Vereecke, G.; Genet, M. J.; Bertrand, P.; Stone, W. E. E.; *Surf. Interface Anal.* **1993**, *20*, 179.
 16. Bychkov, V. Yu.; Sinev, M. Yu.; Korchak, V. N.; Aptekar, E. L.; Krylov, O. V. *Kinet. Catal. (Engl. Transl.)* **1989**, *30*, 989.
 17. Shamilov, N. T.; Vislovskii, V. P. *J. Korean Chem. Soc.* **2011**, *55*(1), 81.
 18. Morterra, C.; Magnacca, G. *Catal. Today* **1996**, *27*, 497.
 19. Wachs, I. E. *Catal. Today* **1996**, *27*, 437.
 20. Topsøe, N.-Y. *J. Catal.* **1991**, *128*, 499.
 21. Busca, G.; Ricchiardi, G.; SiewHew Sam, D.; Volta, J.-C.; *J. Chem. Soc. Farad. Trans.* **1994**, *90*, 1161.
 22. Takagi, M.; Kawai, T.; Soma, M.; Onishi, T.; Tamaru, K.; *J. Catal.* **1977**, *50*, 441.
 23. Belokopytov, Y. V.; Kholyavenko, K. M.; Gerei, S. V. *J. Catal.* **1979**, *60*, 1.
 24. Centeno, M. A.; Benites, J. J.; Malet, P.; Carrizosa, I.; Odriozola, J. A.; *Appl. Spectroscopy* **1997**, *51*, 416.
 25. Dines, T. J.; Rocheste, C. H.; Ward, A. M. *J. Chem. Soc. Faraday Trans.* **1991**, *87*, 653.
 26. Inomata, M.; Mori, K.; Miyamoto, A.; Murakami, Y. *J. Phys. Chem.* **1983**, *87*(5), 761.
 27. Khader, M. M. *J. Mol. Catal. A*, **1995**, *104*, 87.
 28. Sobalik, Z.; Kozlowski, R.; Haber, J. *J. Catal.* **1991**, *127*, 665.
 29. Bychkov, V. Y.; Sinev, M. Y.; Vislovskii, V. P. *Kinet. Catal. (Engl. Transl.)* **2001**, *42*, 574.
-